Microstructural evolution induced by heat treatment in the Co28Cr6Mo alloy produced by Selective Laser Melting

L. Tonelli, I. Boromei, E. Liverani, L. Ceschini

Co28Cr6Mo alloy is one of the most widespread biomaterials used for the fabrication of permanent implants that nowadays can be processed by Additive Manufacturing (AM) techniques. In fact, the biomedical field takes great advantages from additive technologies, specifically Selective Laser Melting (SLM), due to the possibility of realizing tailored devices, based on the actual patience needs. Conventional processing routes of this alloy are complex and often require a heat treatment aimed at improving, for example, wear resistance. However, by considering the very fine and peculiar SLM microstructure, heat treatment parameters should be specifically optimized. The present work focused on the investigation of the effects induced by aging treatments in the microstructure of SLM Co28Cr6Mo alloy. The analyses allowed to delineate the evolution occurred in the microstructure as a consequence of thermal exposure and to identify the conditions which determine the complete modification of the as-built microstructure.

KEYWORDS: ADDITIVE MANUFACTURING, SELECTIVE LASER MELTING, POWDER BED FUSION, BIOMATERIALS, MICROSTRUCTURE, HEAT TREATMENT

INTRODUCTION

Nowadays, it is possible to fabricate innovative and patient-specific medical devices by means of Additive Manufacturing (AM) processes [1,2]. In fact, because of the layer-wise manufacturing method that characterizes AM processes like Selective Laser Melting (SLM), three-dimensional parts can be realized without requiring the fabrication of molds or die, as for casting and forging conventional processes, making customization and tailoring of the device economically affordable. By referring to permanent orthopedic implants for joint replacement such as knee and ankle prostheses, they are usually made of the Co28Cr6Mo alloys [3,4] that can assure the high mechanical strength, wear and corrosion resistance required by these specific applications [5]. In case of complex geometries like the femoral or the talar component of knee and ankle prostheses, respectively, the conventional manufacturing is usually carried out by a dedicated investment casting technique followed by a heat treatment, consisting of three main stages: solution treatment (1200-1255°C for 1-3h), followed by water quen-

Lavinia Tonelli, Iuri Boromei, Erica Liverani, Lorella Ceschini
Dipartimento di Ingegneria Industriale (DIN), Università di Bologna, Bologna, Italia

ching and artificial aging (890-900°C) [6]. The purposes of this conventional heat treatment can be synthetized as: i) homogenizing the as-cast microstructure and reducing segregation, ii) promoting the martensitic transformation and inducing precipitation of fine carbide particles [7]. In case of SLM, it should be evidenced that the resulting microstructure diverges substantially from the conventional as-cast one, thus suggesting the need for a specific heat treatment optimization. SLM, in fact, is based on the localized melting of small portions of fine metallic powders that solidify very rapidly and in conditions far from the equilibrium, as a consequence a very fine and metastable supersaturated microstructure is formed in the as-built alloy [8,9]. Therefore, heat treatment should be designed by taking into consideration these specific microstructural features and, possibly, avoiding coarsening of this very fine microstructure. At present, literature works on heat-treated Co28Cr6Mo SLM alloy have been focused on the high-temperature (1150-1220°C) solution treatment with and without a subsequent aging treatment (750-900°C) [10–13], and on long-time annealing (750-1150°C) [14]. Due to the lack of data on short-time heat treatment, able to avoid excessive coarsening of the SLM microstructure, in the present work the high-temperature solution treatment was eliminated and only direct aging was performed, by exploiting the potential of the supersaturated solid solution resulting from SLM. Experimental analyses were focused on the microstructural modifications induced by low temperature (600-900°C) and short-time (30-180 min) aging treatment applied to the Co28Cr6Mo SLM alloy. The modifications occurring in the microstructure as a consequence of thermal exposure have been traced and the effect on the main microstructural features has been outlined by means of microstructural analyses.

MATERIALS AND METHODS

Samples in form of blocks (6x20x30 mm^3) were produced by SLM with a vertical building direction in a nitrogen atmosphere starting from Co28Cr6Mo spherical powder whose composition complied with the ASTM F75 [3]. A SLM Sisma MySynt 100 machine was used adopting process parameters disclosed in Table 1. Parameters were determined in order to obtain values of Laser Energy Density (LED) closed to the optimized one, as discussed in a previous work [15]. LED is obtained as a combination of laser power (P), scanning velocity (v), hatch distance (h), layer thickness (d) from the formula LED = P (v **x** h x d)$^{-1}$.

Tab.1 -Process parameters used for the fabrication of SLM Co28Cr6Mo samples

Laser Power [W]	Scanning velocity [mm s-1]	Layer Thickness [mm]	Hatching Space [mm]	LED [J mm-3]
90-130-150	900-500-1100	0.02	0.04-0.06-0.08	120-125-163-70

Direct aging treatments of the as-built samples were performed in the range 600-900 °C with a soaking time from 30 to 180 min in a muffle furnace operating at ambient atmosphere. Aging treatments were firstly carried out on samples obtained with the lower values of LED (120 and 125 J mm^{-3}), and then they were repeated also for samples with the higher LED (163 and 170 J mm^{-3}), with the aim to verify repeatability. Microstructural characterization was performed via optical (OM) and scanning electron (SEM) microscopy equipped with Energy Dispersive X-ray Spectroscope (EDS) on sections parallel to the building direction. Prior to microstructural investigation, sections were embedded in a phenolic resin and subjected to a standard metallographic preparation followed by electrochemical etching in a water-based solution of hydrochloric acid and ferric chloride, as described in [16].

RESULTS AND DISCUSSION

As shown in Figure 1, additive processes like SLM result in a hierarchical microstructure composed by: i) a layered structure made by successive melt pools representing the localized fusion zones; ii) columnar grains crossing-over layers formed by epitaxy, iii) a very fine solidification substructure inside melt pools, cellular in case of Co28Cr6Mo alloy [8,15,17]. Such microstructural features can be observed by using different metallographic analyses: i) melt pools, whose size is usually in the order of hundreds of micrometers, can be clearly observed by bright field optical microscopy; ii) epitaxial grains, whose width is in the order of tens of micrometers, are highlighted by polarized light microscopy; iii) the very fine cellular sub-structure, whose cells have a sub-micrometer size, that can be resolved only by electron microscopy. The cellular sub-structure is comprised of Co-based cells surrounded by a fine network formed by segregation of alloy elements, mainly Mo, whose formation phenomena were described by [9].

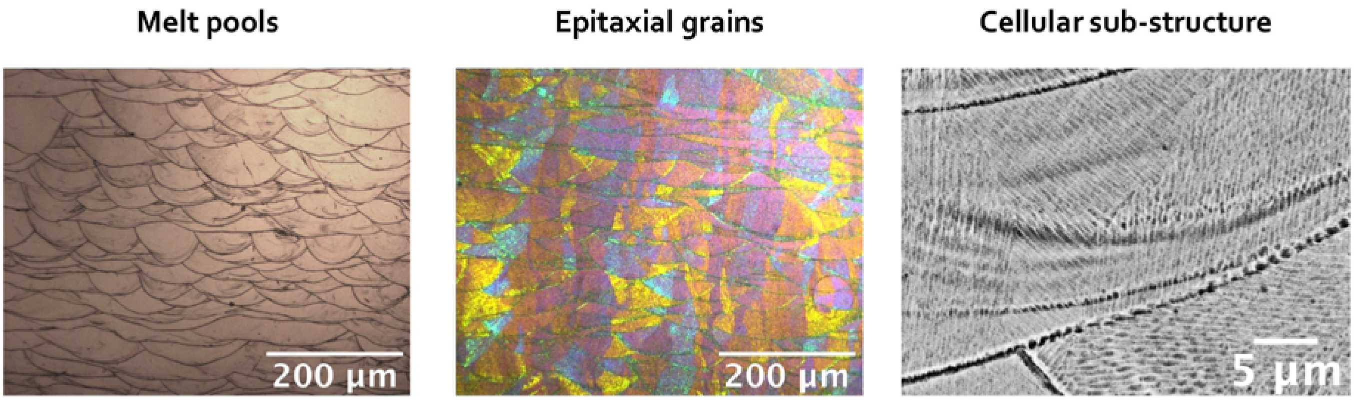

Fig.1 - Micrographs showing the different features forming the hierarchical microstructure of SLM Co28Cr6Mo as-built alloy / Micrografie ottiche della lega Co28Cr6Mo processata con SLM allo stato non trattato: evidenza dei diversi elementi che costituiscono la microstruttura gerarchica.

MELT POOLS EVOLUTION

A first assessment of the microstructural evolution due to the exposure at high temperatures is represented by optical analyses at low magnification reported in Figure 2, where solidified melt pools can be analyzed. The lowest aging temperature (600°C) did not significantly affect the as-built microstructure, even at the longest soaking time of 180 min. In fact, melt pools are clearly visible in the micrographs. Melt pools were unaffected also by aging treatment performed at 700°C up to 90 min, while after 180 min at this temperature a new feature in the microstructure was revealed, showing vertical lines crossing-over layers, while solidified melt pools could be still distinguished in the background. As also showed in Figure 3, it appeared that such lines corresponded to borders of epitaxial grains crossing over layer that were presumably affected by the applied aging treatment (700°C for 180 min). Aging treatment at 800°C induced modifications in the microstructure even after a short treatment time (30 min) and, similarly to aging at 700°C for 180 min, borders of epitaxial grains were slightly evidenced. Additionally, the presence of new linear features inclined by approx. ±45° inside melt pools was noticed, evidenced by white arrows in Figure 2. The area occupied by these linear features increased by increasing soaking time and after the 180 min treatment at 800°C they became the predominant element in the microstructure. Analogous considerations can be also discussed for the 900°C aging treatment, with the main difference that linear elements progressively decreased with an increase of the aging time, and vanished after the 180 min treatment. It should be noticed that, with the only exception of the 900°C for 180 min treatment, solidified melt pools were always clearly recognizable in the microstructure. It is therefore presumable that no complete recrystallization of the microstructure occurred. The occurrence of recrystallization and homogenization was in fact evidenced by other authors in case of high temperatures treatments (1150-1220°C) [10,11,13,18].

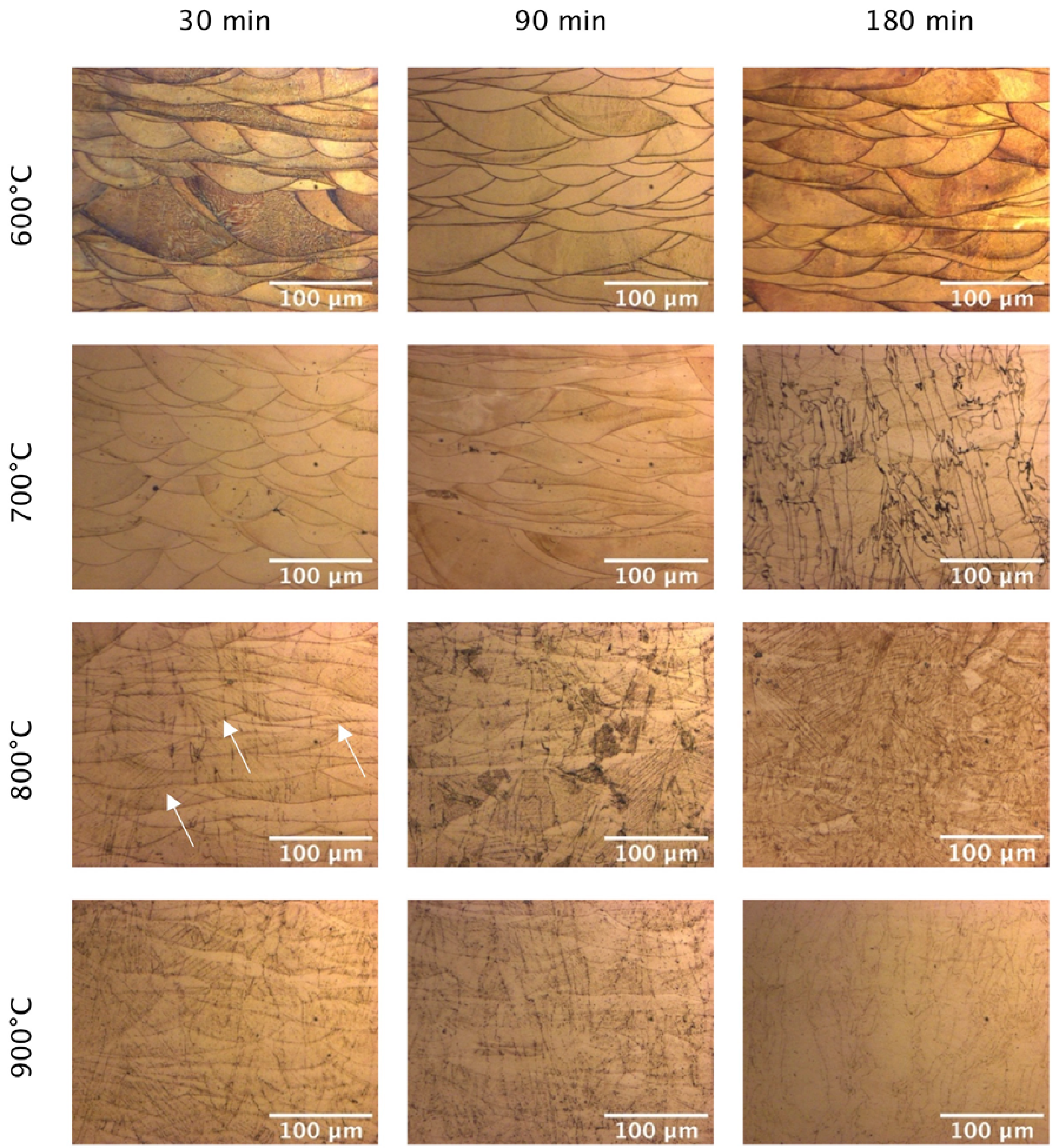

Fig.2 - Optical micrographs of SLM Co28CCr6Mo samples subjected to direct aging treatments in the range 600-900°C for 30-180 min / Micrografie ottiche della lega Co28Cr6Mo processata con SLM e sottoposta a trattamenti di invecchiamento diretto nell'intervallo 600-900°C per tempi da 30 a 180 min.

EPITAXIAL GRAINS EVOLUTION

The evolution of epitaxial grains, observed by polarized light microscopy, is shown in Figure 3 for some representative heat treatment conditions. The 700°C for 180 min treatment still preserved grains and, from a direct comparison with the bright field micrograph obtained in the same conditions and reported in Figure 2, it is possible to confirm that vertical lines crossing-over layer corresponded to epitaxial grains borders. Then, by increasing aging temperature and time, epitaxial grains were progressively less defined and, after holding at 900°C for 180 min, were no longer clearly identifiable. In addition, from the observation of the microstructure obtained after aging treatment at 800°C for 90 min, it can be noticed that the aforementioned linear features oriented at approx. ±45°, that appeared after aging treatments performed at 800°C, laid inside epitaxial grains, as indicated by arrows in Figure 3.

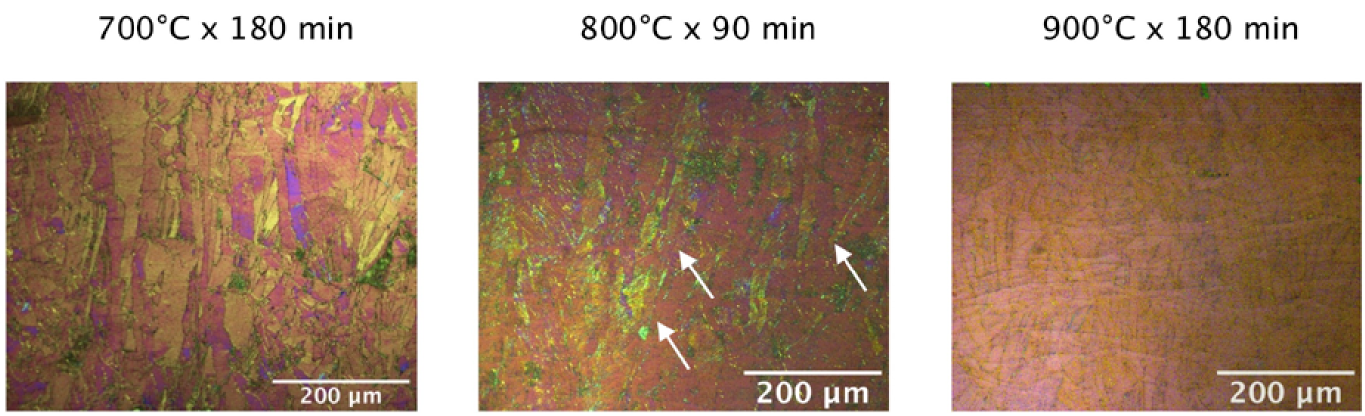

Fig.3 - Polarized light micrographs comparing of representative heat-treated SLM samples in which epitaxial grains crossing-over layer are highlighted / Micrografie ottiche in luce polarizzata in cui si evidenziano i grani epitassiali che attraversano i layer, confronto tra diverse condizioni di trattamento termico rappresentative

CELLULAR SUB-STRUCTURE EVOLUTION

High magnification SEM microscopy is needed in order to reveal the aforementioned extremely fine cellular substructure inside the solidified melt pools (Figure 4). As previously discussed, major microstructural modifications, as appreciable by optical analyses, occurred at temperatures above 700°C, thus in Figure 4 only the 700, 800 and 900°C treatments are compared. Up to the 800°C for 90 min treatment, cellular sub-structure could be identified in the micrographs, the same disappeared for treatments performed at higher temperatures and for longer soaking time. From the 700°C for 180 min treatment, it appeared that the cellular sub-structure progressively developed in the formation of globular particles, starting from epitaxial grains boundaries and then involving the whole cellular sub-structure. The transformation occurring in the cellular substructure can explain the formation of linear features evidenced inside epitaxial grains by the optical analyses. In case of 800°C for 180 min treatment, sub-micrometric particles were finely and homogeneously distributed in the matrix. In addition, in case of 900°C treatment the density of globular particles decreased, thus suggesting the development of dissolution phenomena.

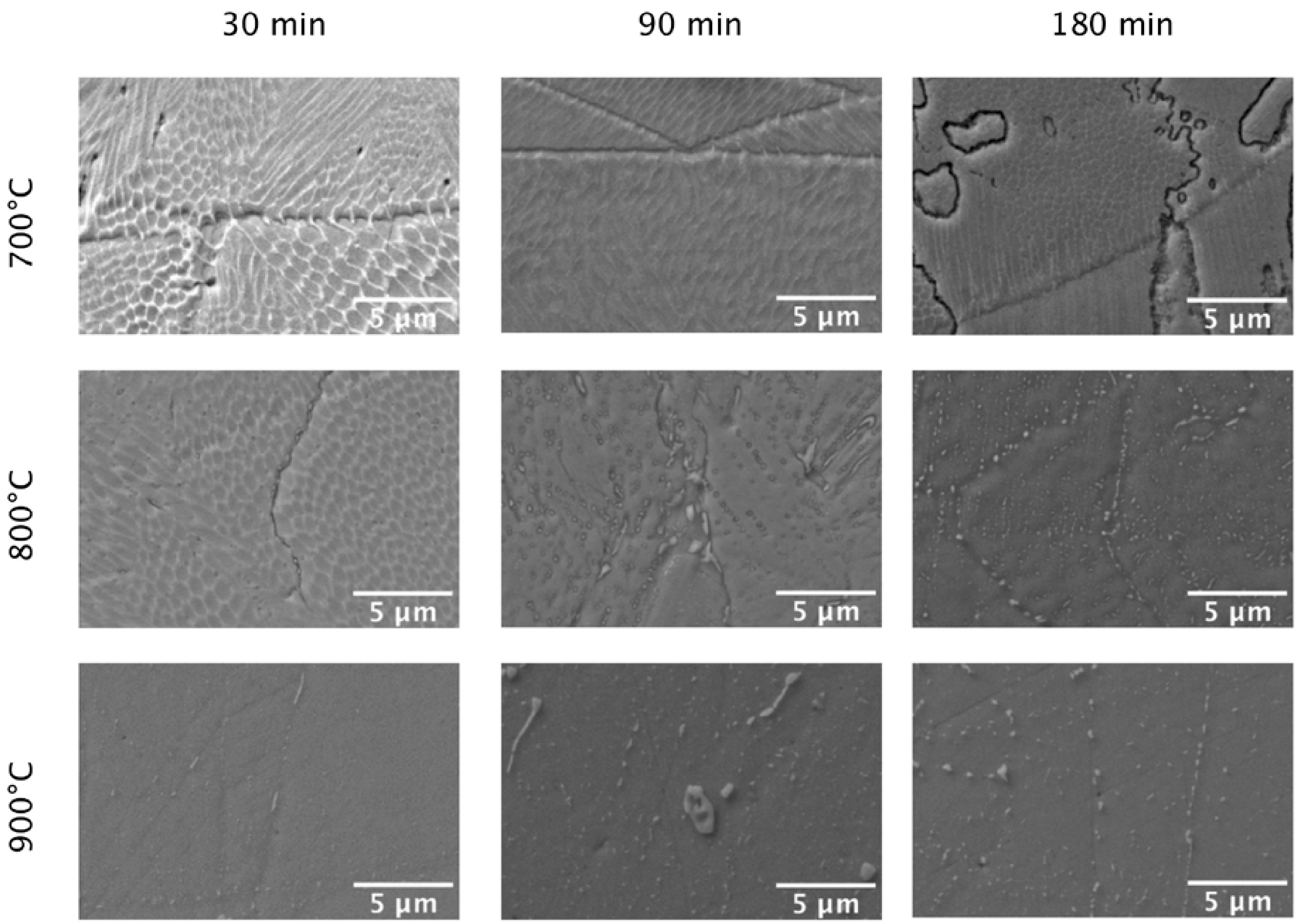

Fig.4 - SEM micrographs of SLM Co28Cr6Mo samples subjected to direct aging treatments in the range 700-900°C for 30-180 min / Micrografie SEM della lega Co28Cr6Mo processata con SLM e sottoposta a trattamenti di invecchiamento nell'intervallo 700-900°C per tempi da 30 a 180 min.

Semi-quantitative compositional analyses on the sub-micrometric globular particles (Figure 5) were performed via SEM-EDS. In correspondence of such particles (Spectra 1 and 2), an enrichment of some of the alloy elements (Si, C and Mo) was found with respect to the matrix (Spectra 3), that complied with the requirement given by the ASTM F75 Standard [3]. As already mentioned, literature reports Mo and C segregation along cellular boundaries of the as-built microstructure [12,19] and this aspect was also evidenced in the present work by SEM-EDS analyses on as-built alloy in Figure 5. Hence, SEM-EDS results confirmed that globular particles originated from cellular sub-structure and, more specifically, from the network constituted by cell borders that presumably broke up as a consequence of thermal exposure, similarly to what happens in case of others SLM processed alloys like the Al-Si ones [20,21]. Finally, as a confirmation of the repeatability of effects of aging treatments, it is worth mentioning that the above discussed microstructural modifications occurred in the samples obtained with both considered LED ranges (approx. 120 and 170 J mm^{-3}).

Heat-treated

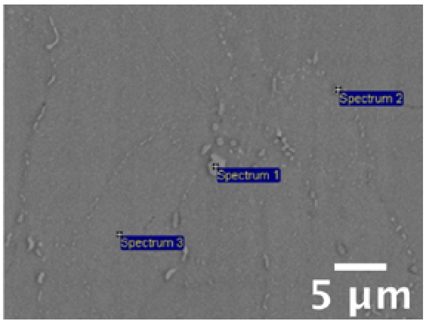

Spectrum	Elements (wt.%)					
	C	Si	Cr	Mo	Mn	Co
1	3.54	1.80	27.16	9.90	0.74	56.86
2	4.28	1.70	27.28	9.31	0.94	56.49
3	3.29	0.83	27.48	6.09	0.91	61.40

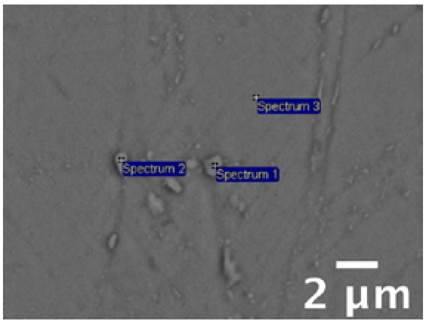

Spectrum	Elements (wt.%)					
	C	Si	Cr	Mo	Mn	Co
1	4.21	1.56	32.70	8.16	0.89	52.48
2	4.09	1.54	30.70	8.21	1.10	54.36
3	2.49	0.77	27.92	6.38	1.09	61.35

As-built

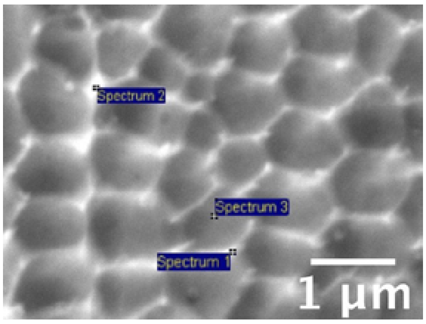

Spectrum	Elements (wt.%)					
	C	Si	Cr	Mo	Mn	Co
1	3.25	0.71	28.22	5.99	0.94	60.90
2	5.65	0.89	27.65	7.38	0.76	57.67
3	-	0.94	29.00	5.70	0.95	63.40

Fig.5 - SEM-EDS analyses conducted on globular particles (Spectra 1 and 2) formed after aging treatment of the SLM Co28Cr6Mo alloy, compared to the matrix (Spectrum 3) / Analisi SEM-EDS delle particelle globulari (Spettri 1 and 2) formatesi a seguito del trattamento di invecchiamento della lega Co28Cr6Mo processata con SLM, confrontate con la matrice (Spettro 3).

CONCLUSIONS

The present work focused on the investigation of the microstructural evolution occurred during direct aging treatment of the Co28Cr6Mo alloy produced by Selective Laser Melting (SLM). Aging treatments were performed in the range 600-900°C for a holding time between 30 and 180 min. The microstructural investigation by means of optical and scanning electron microscopy led to the following conclusions:

- For a given time-temperature combination, aging treatments affected one or more microstructural features characterizing the typical hierarchical SLM microstructure (comprised of successive melt pools, epitaxial grains crossing-over layers, a very fine solidification cellular substructure), starting from 700 °C aging treatment.
- Trace of the solidified melt pools were preserved for all treatments up to 900°C x 90 min; only after aging treatment at 900°C for 180 min they disappeared.
- Epitaxial grains crossing-over layers were the first micro-

structural feature affected by the heat treatment; starting from a permanence of 180 min at 700°C and for all treatment time at higher temperatures, grains boundaries were involved in the formation of fine globular particles.

- From aging treatment at 700°C for 180 min, cellular sub-structure progressively disappeared and after 90 min permanence at 800°C, and for any soaking time at 900°C, it was no longer observable in the microstructure.

- As a consequence of the thermal exposure, the as-built sub-structure, consisting of very fine cells surrounded by a network of segregated alloys elements, evolved in the formation of fine globular particles dispersed in the matrix, starting from epitaxial grains borders and then involving the entire microstructure. In correspondence of such particles, enrichment of alloy elements was evidenced.

REFERENCES

[1] M. Lowther, S. Louth, A. Davey, A. Hussain, P. Ginestra, L. Carter, N. Eisenstein, L. Grover, S. Cox, Clinical, industrial, and research perspectives on powder bed fusion additively manufactured metal implants, Addit. Manuf. 28 (2019) 565–584. doi:10.1016/j.addma.2019.05.033.

[2] L. Bai, C. Gong, X. Chen, Y. Sun, J. Zhang, L. Cai, S. Zhu, S.Q. Xie, Additive manufacturing of customized metallic orthopedic implants: Materials, structures, and surface modifications, Metals (Basel). 9 (2019) 1–26. doi:10.3390/met9091004.

[3] ASTM F75-18, Standard Specification for Cobalt-28 Chromium-6 Molybdenum Alloy Castings and Casting Alloy for Surgical Implants (UNS R30075), (2018). doi:https://doi.org/10.1520/F0075-12.

[4] ASTM F1537-20, Standard Specification for Wrought Cobalt-28Chromium-6Molybdenum Alloys for Surgical Implants (UNS R31537, UNS R31538, and UNS R31539), (2020). doi:10.1520/F1537-20.

[5] Q. Chen, G.A. Thouas, Metallic implant biomaterials, Mater. Sci. Eng. R Reports. 87 (2015) 1–57. doi:10.1016/j.mser.2014.10.001.

[6] R. Narayan, ASM Handbook, Volume 23, Materials for Medical Devices, ASM International, 2012.

[7] R. Pillar, S.D. Ramsay, Cobalt-base alloys, in: R.J. Narayan (Ed.), Mater. Med. Devices, ASM Interbational, 2012: pp. 211–222. doi:10.31399/asm.hb.v23.a0005669.

[8] T. DebRoy, H.L. Wei, J.S. Zuback, T. Mukherjee, J.W. Elmer, J.O. Milewski, A.M. Beese, A. Wilson-Heid, A. De, W. Zhang, Additive manufacturing of metallic components – Process, structure and properties, Prog. Mater. Sci. 92 (2018) 112–224. doi:10.1016/j.pmatsci.2017.10.001.

[9] K.G. Prashanth, J. Eckert, Formation of metastable cellular microstructures in selective laser melted alloys, J. Alloys Compd. 707 (2017) 27–34. doi:10.1016/j.jallcom.2016.12.209.

[10] S.M.J. Razavi, A. Avanzini, G. Cornacchia, L. Giorleo, F. Berto, Effect of heat treatment on fatigue behavior of as-built notched Co-Cr-Mo parts produced by Selective Laser Melting, Int. J. Fatigue. 142 (2021) 105926. doi:10.1016/j.ijfatigue.2020.105926.

[11] S.L. Sing, S. Huang, W.Y. Yeong, Effect of solution heat treatment on microstructure and mechanical properties of laser powder bed fusion produced cobalt-28chromium-6molybdenum, Mater. Sci. Eng. A. 769 (2020) 138511. doi:10.1016/j.msea.2019.138511.

[12] C. Song, M. Zhang, Y. Yang, D. Wang, Y. Jia-kuo, Morphology and properties of CoCrMo parts fabricated by selective laser melting, Mater. Sci. Eng. A. 713 (2018) 206–213. doi:10.1016/j.msea.2017.12.035.

[13] M. Béreš, C.C. Silva, P.W.C. Sarvezuk, L. Wu, L.H.M. Antunes, A.L. Jardini, A.L.M. Feitosa, J. Žilková, H.F.G. de Abreu, R.M. Filho, Mechanical and phase transformation behaviour of biomedical Co-Cr-Mo alloy fabricated by direct metal laser sintering, Mater. Sci. Eng. A. 714 (2018) 36–42. doi:10.1016/j.msea.2017.12.087.

[14] Y. Kajima, A. Takaichi, N. Kittikundecha, T. Nakamoto, T. Kimura, N. Nomura, A. Kawasaki, T. Hanawa, H. Takahashi, N. Wakabayashi, Effect of heat-treatment temperature on microstructures and mechanical properties of Co–Cr–Mo alloys fabricated by selective laser melting, Mater. Sci. Eng. A. 726 (2018) 21–31. doi:10.1016/j.msea.2018.04.048.

[15] L. Tonelli, A. Fortunato, L. Ceschini, CoCr alloy processed by Selective Laser Melting (SLM): effect of Laser Energy Density on microstructure, surface morphology, and hardness, J. Manuf. Process. 52 (2020) 106–119. doi:10.1016/j.jmapro.2020.01.052.

[16] D. Klarstrom, P. Crook, J. Wu, Metallography and Microstructures of Cobalt and Cobalt Alloys, in: G.F. Vander Voort (Ed.), Metallogr. Microstruct. - ASM Handb. Vol.9, ASM International, 2004: pp. 762–774. doi:10.31399/asm.hb.v09.a0003771.

[17] L. Tonelli, I. Boromei, A. Fortunato, L. Ceschini, Selective Laser Melting of a CoCrMo alloy for biomedical applications: Correlations between microstructure and process parameters, Metall. Ital. 111 (2019) 41–47.

[18] M. Zhang, Y. Yang, C. Song, Y. Bai, Z. Xiao, An investigation into the aging behavior of CoCrMo alloys fabricated by selective laser melting, J. Alloys Compd. 750 (2018) 878–886. doi:10.1016/j.jallcom.2018.04.054.

[19] B. Qian, K. Saeidi, L. Kvetková, F. Lofaj, C. Xiao, Z. Shen, Defects-tolerant Co-Cr-Mo dental alloys prepared by selective laser melting, Dent. Mater. 31 (2015) 1435–1444. doi:10.1016/j.dental.2015.09.003.

[20] R. Casati, M.H. Nasab, V. Tirelli, M. Vedani, Effect of different heat treatment routes on microstructure and mechanical properties of AlSi7Mg, AlSi10Mg and Al-Mg-Zr-Sc alloys produced by selective laser melting, Euro PM 2018 Congr. Exhib. (2020).

[21] F. Trevisan, F. Calignano, M. Lorusso, J. Pakkanen, E.P. Ambrosio, L. Mariangela, M. Pavese, D. Manfredi, P. Fino, Effects of heat treatments on A357 alloy produced by selective laser melting, World PM 2016 Congr. Exhib. (2016).and impact toughness of AlSi-9Cu3(Fe) diecasting alloys, Materials Science and Engineering A, 603, (2014), 58-68.

[23] E.J. Vinarcik, High Integrity Die Casting Processes; JohnWiley& Sons: New York, NY, USA, 2003, pp. 162-168.